11

Fatigue Characterization of Fiber/Metal Laminates

Y. TOI and Y. FUJIWARA
Aerospace Division
Fuji Heavy Industries, Ltd.
Utsunomiya, Japan

ABSTRACT

High performance aircraft in the future need more damage tolerant materials and optimized designs. In SSTs, the prevention of lethal rapid decompression in high altitude operations is one of the issues for the structural design of the fuselage. In meeting this requirement, fiber/metal laminates are considered as one of the candidates. Fiber/metal laminates show the attractive feature of slow crack growth. So far, one problem for structural designers in the application of fiber/metal laminates has been that the estimation of crack growth is too complex and has limited generality. A new simple approach is proposed with coupon test results with Glares. Assuming a monolithic thickness and that the surface cracks go through the thickness, the modified stress intensity factor (ΔK_{mod}) is introduced with the basic stress intensity factor (ΔK) multiplied by the modification factor (β_{fb}). The modification factor β_{fb} can be defined by just the crack size. The current analytical practice for aluminum alloys is effective for fiber/metal laminates with ΔK_{mod}. This approach is a practical way to understand the performance limit of fiber/metal laminates and is effective in the development of new types of fiber/metal laminates.

1. INTRODUCTION

One of the issues in the structural design of the SST fuselages is the prevention of lethal rapid decompression in high altitude operations. The problems of multi-site cracks in the current aging transports will be more critical in SSTs. Sudden link-ups of small cracks and the isolations by flapping mechanism may be accepted in structural design, but should be avoided in view of the medical dangers of rapid decompression. In meeting this requirement, the high fatigue resistance of fiber/metal laminates is very attractive and fiber/metal laminates are considered to be one of the candidates for the next generation SST fuselage.

Fiber/metal laminates consist of alternating layers of thin metal sheets and fiber reinforced plastic sheets. Through extensive development studies by Delft University, Structural Laminates Company and other researchers, aircraft applications for the production parts of the secondary structures have been started and evaluation tests for the primary structures are being conducted now.

The crack growth rates in fiber/metal laminates are much slower than in conventional aluminum alloys. The basic mechanism of this slow crack growth is explained by 'fiber bridging' at the crack tip. Local delaminations between metal sheets and fiber layers or delaminations in fiber layers around the crack tips relieve the stress concentration of fibers. Shear deformation of the adhesive between metals and fibers also relieve the fiber stresses. The crack growth depends on the balance of strength and stiffness between fibers and adhesives. Schijve[1] explained the basic mechanism well in his report. Marissen[2] developed a break down analysis model to describe the process of crack growth in fiber/metal laminates (for ARALL Laminates).

So far, one engineering drawback in the application of fiber/metal laminates has been that the mechanism of the fiber bridging is too complex and the properties show limited generality. The purpose of this study is to develop a simpler and more practical estimation method for the crack growth of fiber/metal laminates. Crack propagation tests have been conducted with Glares, which is one of the commercially available fiber/metal laminates from Structural Laminates Company. Through the evaluation of the test results, a simple empirical crack growth model has been derived.

2. CRACK PROPAGATION TESTS

2.1 TEST SPECIMENS AND PROCEDURE

Glare is one of the commercially available types of fiber/metal laminates made by Structural Laminates Company. It consists of 2024-T3 aluminum alloy sheets and fiberglass tapes. Fiberglass layers are not post-stretched.

All test items are summarized in Table 1. In the crack propagation tests, the center cracked tension specimens made of four types of Glares were tested with four levels of constant amplitude cyclic loads at room temperature. Two types of initial starter notches are prepared at the center hole; one is the through-saw cut and the other is the corner-saw cut (one surface only). The size of the saw cuts was about 1mm to 2mm.

One multiple-site-cracks specimen which had no initial starter notches was also tested at the lowest stress level. The stress ratio was 0.05, and the cyclic loading speed was 5Hz in all tests. Residual strength tests were carried out for some specimens subsequent to the crack propagation tests.

All specimens had the same shape as shown in Fig. 1. The tests with the specimens with corner cracks and all Glare2 were carried out at Yokohama National University and the others at Fuji Heavy Industries. The crack length on both sides of the metal surfaces was measured by magnifying glasses.

See Fig.2 for the test set-up condition.

2.2 TEST RESULTS

An example of test results (a-N curve) is shown in Fig.3. Even when the crack length became longer, the crack growth rate did not rapidly increase. In some cases, crack growth rates looked constant and in other cases seemed to slow down.

The condition of the delamination and the broken fibers in typical specimens was examined by chemical etching (Fig.4). The results of etching show that major delaminations exist between the adhesive layers and the fiberglass layers. The cracks on the adhesive layer next to the surface aluminum layer reaches the crack tips of the surface. But most of the fibers look intact. Inside metal sheets have cracks which almost reach the surface crack tips. Delaminations in the fiberglass layers are not clearly found.

In the corner crack tests, the visible cracks at the reverse side of the starter notch side were nucleated comparatively earlier and followed the reverse side cracks. Difference in crack propagation rates da/dN between the through-saw cuts and the corner-saw cuts was sufficiently small(Fig.5).

The multiple-site crack propagation test was carried out until all of the cracks were linked up on the surface. The cracks were nucleated at both edges of all holes.

Nucleation was earlier than expected, but crack propagation was slow and not accelerated until the end of the test. After the surface cracks linked up, the specimen did not break away, and the remaining fiber layers sustained the loads. An example a-N curve of the center hole in the multiple-site-cracks specimen is shown in Fig.6.

The results of the residual strength test show clearly that not all fibers were broken along the crack of the metal layer(Fig.7).

3. REVIEW OF SLOW CRACK GROWTH MODEL

The schematic illustration of the fiber bridging at the crack tips is described in Fig.8. The break down analysis model developed by Marissen[2] is the basis for discussing the fiber bridging. One of the key equations is

$$K_{1a} = (S_{1a} - C_{b/a} \times S_{br}) \times (\pi \times a)^{1/2}$$

where

K_{1a}; stress intensity factor in fiber/metal laminate

S_{la} ; remote stress in the total laminate

$C_{b/a}$; correction factor on the efficiency of the crack bridging stresses , related to the axis ratio of the delamination

S_{br}; crack bridging stress calculated over the thickness of laminate.

a; half crack length

A schematic illustration of the equation is shown in Fig.9. Actually, the term of ' $C_{b/a} \times S_{br}$' is not easy to determine. Complex effects of shear deformation of the adhesive (elastic /plastic), delamination growth and fiber strength are condensed into the term.

4. AN EMPIRICAL CRACK GROWTH MODEL

At first, the same evaluation approach to the metal sheets is tried on the Glare test results. Assuming that the laminates are monolithic in thickness and that the surface cracks go through the thickness, the apparent stress intensity factors (ΔK) for laminates are calculated. Fig.10 (a), (c) and (e) show the relations between the crack growth rate da/dN and the apparent ΔK each for Glare 2-3/2, Glare 3-3/2 and Glare 4-3/2. In this approach, da/dN characteristics are not specified only by the ΔK. Data seem to vary with the stress levels.

Then, the modified stress intensity factor (ΔK_{mod}) is introduced by the apparent stress intensity factor (ΔK) multiplied by the modification factor (β_{fb}). The flow to determine β_{fb} is shown in Fig.11. 'ΔK_{mod}' is intended to show the actual ΔK on the aluminum surface foil of the fiber/metal laminate, which is the 2024-T3 sheet. The interesting results obtained by this approach is that the β_{fb} shows a definitive correlation to the crack length 'a'. Several test results at different stress levels tend to fall along one functional line. The summary of the obtained β_{fb} data for Glares is shown in Fig.12, and the curves which best fit the data points of β_{fb} are shown in Fig.13. The effectivity of the β_{fb} can be found clearly in Fig.10(b), (d) and (f). Crack growth rates da/dN of fiber/metal laminates become available to the designer's hand by using the ΔK_{mod}.

Crack growth analysis of fiber/metal laminates is easily conducted by the conventional Paris Law.

$$da/dN = C \times (\Delta K_{mod})^m$$
$$= C \times (\beta_{fb} \times \Delta\sigma_{la} \times (\pi \times a)^{1/2})$$

C, m ; material constant in Paris Law
(same as for 2024-T3 in Glares)

$\Delta\sigma_{la}$; average laminate stress range

An example comparison with the test data and the analysis with the above simplified equation is shown in Fig.14. Generally, good correlation is shown. A back-life from the crack length a= 60mm is compared. Back-life estimation is one of the practical engineering methods in damage tolerant analysis for current commercial airplanes . The differences after 600,000 cycles are thought to be due to the effect of the initial starter notch and the initial specific delamination growth mechanism.

5. CONCLUSIONS

Fiber/metal laminates have the attractive features of extremely slow crack growth, but the mechanism of fiber bridging is too complex for designers.

A simple empirical approach has been developed. With the modification factor β_{fb} applied to the stress intensity factors, da/dN of fiber/metal laminates become available to the designer's hand. This approach is a practical way to understand the performance limit of fiber/metal laminates and is effective in the development of new types of fiber/metal laminates.

The effect of spectrum loadings is not covered here. But the approach developed herein will be a good baseline from which to discuss the phenomena.

ACKNOWLEDGMENT

The work herein has been conducted under a joint research program with the National Aerospace Laboratory. The authors appreciate Dr. Asada for his lead in this program, and Dr. Shimokawa for effective suggestions. Part of the tests were conducted at the Yokohama National University. The authors appreciate Dr. Ishizuka for test efforts and suggestions. The authors wish to express their appreciation to Dr. Verbruggen and Dr.Roebroeks in SLC for their helpful suggestions.

REFERENCES

1 Schijve, J., "Development of fiber-metal laminates, ARALL and Glare, new fatigue resistant materials", Report LR-715, Faculty of Aerospace Engineering, Delft University of Technology, The Netherlands, January 1993.

2 Marissen, R., "Fatigue Crack Growth in ARALL, a Hybrid Aluminum-Aramid Composite Material", Report LR-574,Faculty of Aerospace Engineering, Delft University of Technology, The Netherlands, June 1988.

Table 1 Summary of all test items

<MATERIALS>

FIBER/METAL LAMINATES	FIBER, FIBERGLASS (S-2 0R EQUIVALENT)	METAL Al
GLARE 2	100% 0° FIBERGLASS	2024-T3
GLARE 3	50% 0°, 50% 90° FIBERGLASS	2024-T3
GLARE 4	70% 0°, 30% 90° FIBERGLASS	2024-T3

<CRACK PROPAGATION TESTS>

TEST SPECIMEN ID	LAMINATE TYPE	CONFIGURATION NO. OF LAYERS (METAL/FIBER)	LAMINATE NOMINAL THICKNESS	NO. OF TEST SPECIMENS
A	GLARE 3	3 / 2	1.12mm	7
B	GLARE 2	3 / 2	1.12mm	6
C	GLARE 4	3 / 2	1.44mm	4
D	GLARE 3	4 / 3	1.62mm	7

<MULTI-SITE CRACK PROPAGATION TESTS>

GLARE3-3/2 5/32IN DIA HOLES WITH 5.8D PITCH	1

<RESIDUAL STRENGTH TESTS>

GLARE3-3/2, GLARE4-3/2, GLARE2-3/2	1 EACH
GLARE3-4/3	2

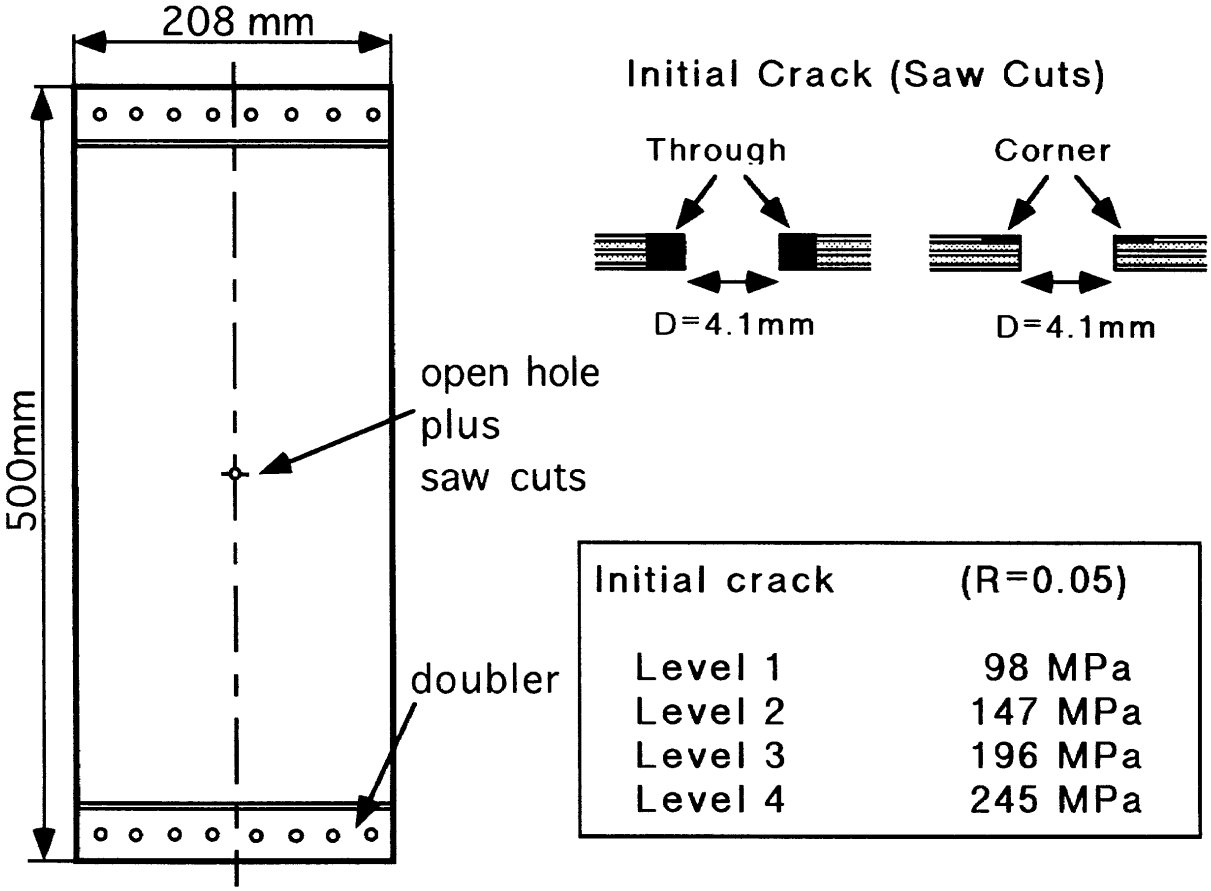

Figure 1 Configuration of the test specimen

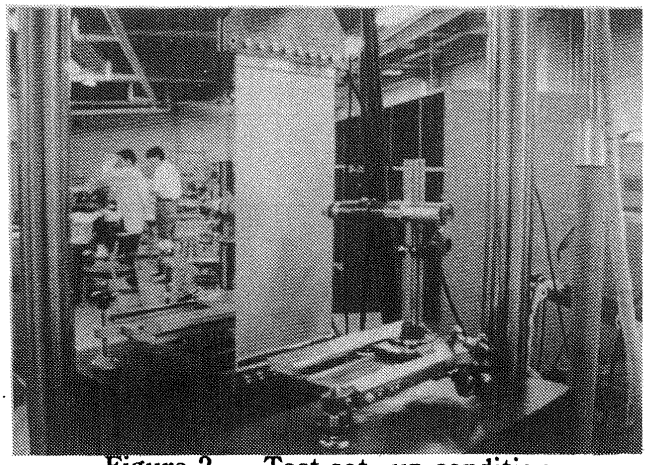

Figure 2 Test set–up condition

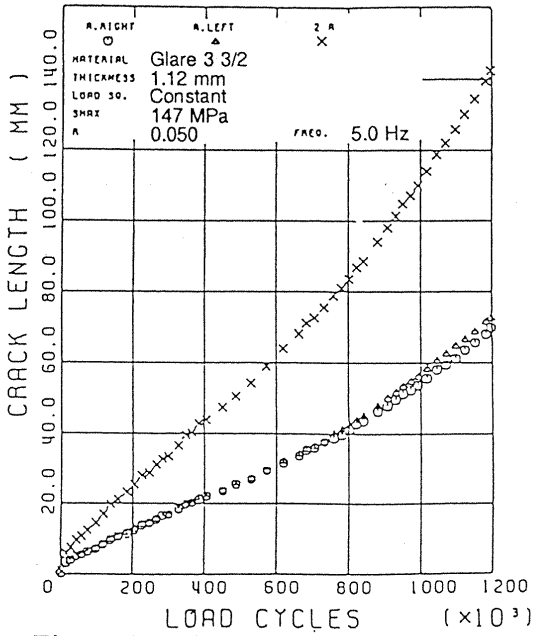

Figure 3 'a–N' Curve in Test A

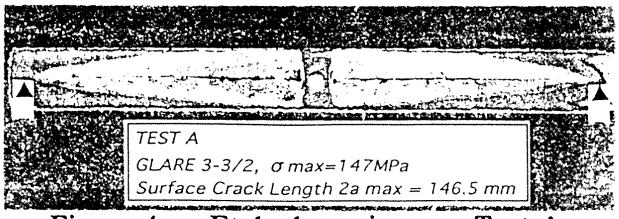

Figure 4 Etched specimen – Test A

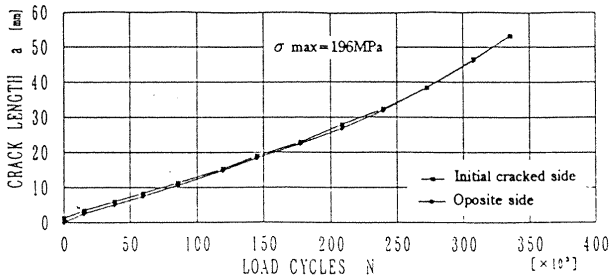

Figure 5 'a–N' Curve of corner saw cut in Test A (Glare3 3/2)

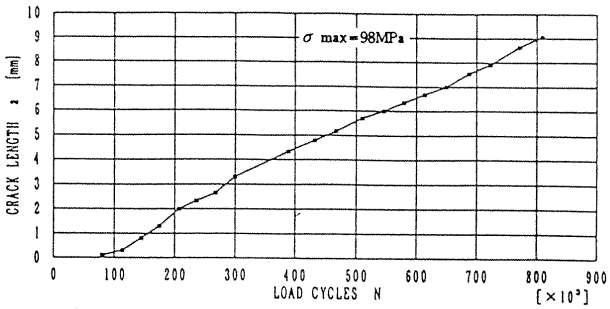

Figure 6 'a–N' Curve of Multiple–site crack in Test A (Glare3 3/2)

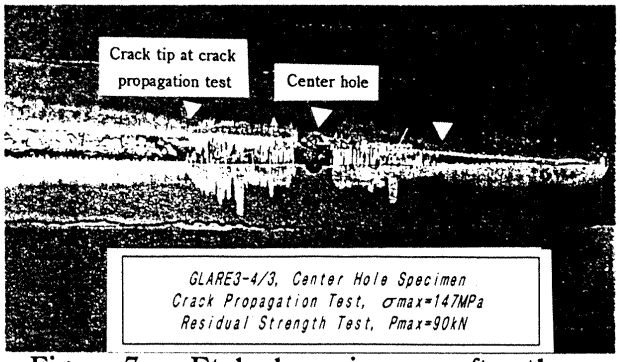

Figure 7 Etched specimen – after the residual strength test

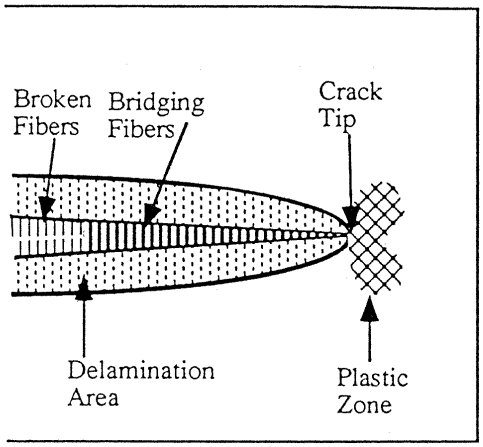

Figure 8 Schematic illustration of fiber bridging at the crack tip in fiber/metal laminates

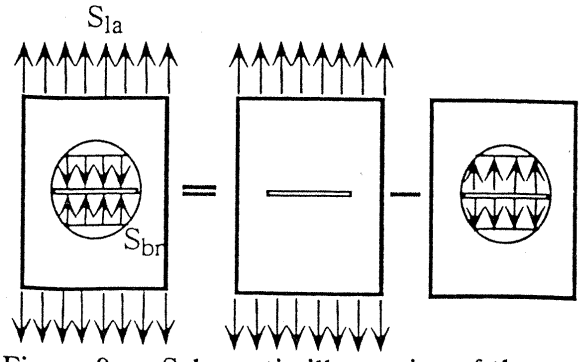

Figure 9 Schematic illustration of the equation

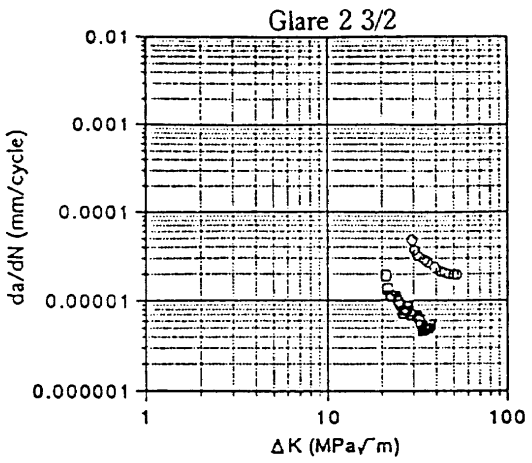

(a) original

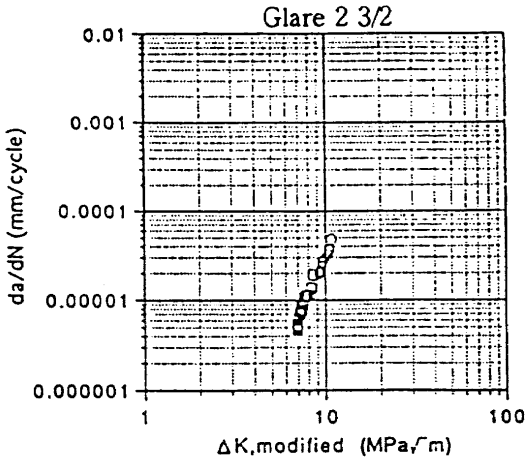

(b) 'β, fiber bridging' applied

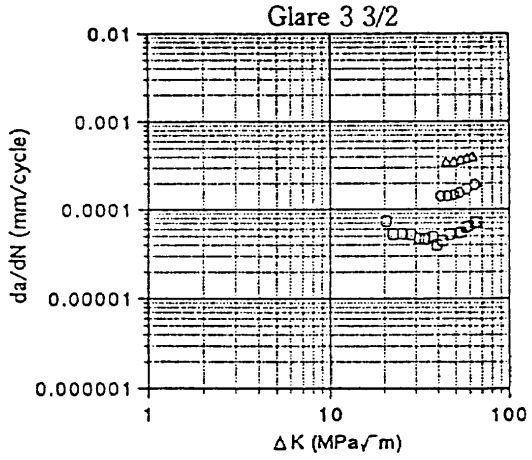

(c) original

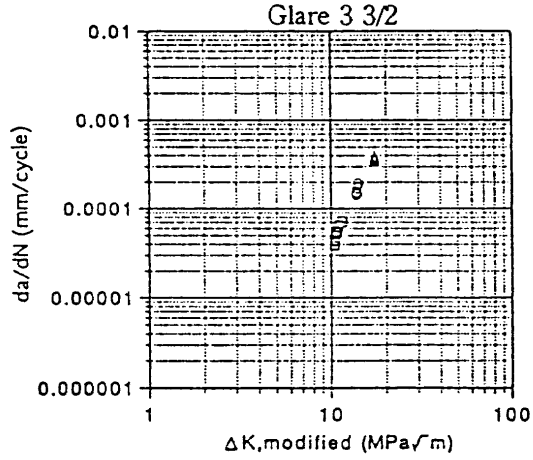

(d) 'β, fiber bridging' applied

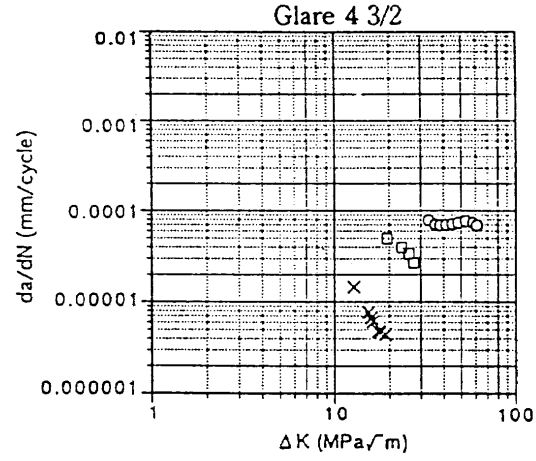

(e) original

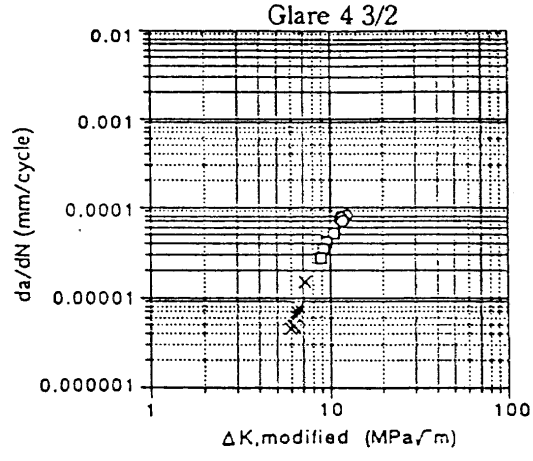

(f) 'β, fiber bridging' applied

× σmax= 98MPa
□ σmax=147MPa
○ σmax=196MPa
△ σmax=245MPa

Figure 10 da/dN vs Δ K or Δ K,modified

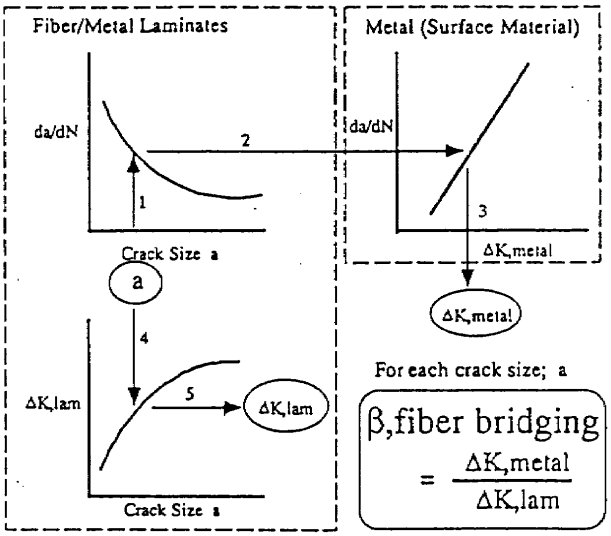

Figure 11 Flow to determine 'β ,fiber bridging'

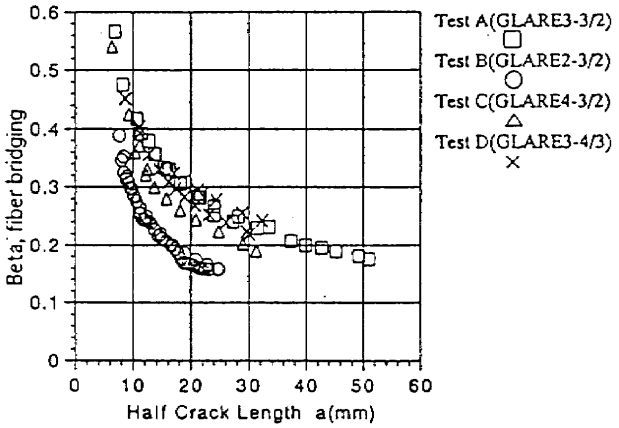

Figure 12 'β ,fiber bridging' obtained from the tests

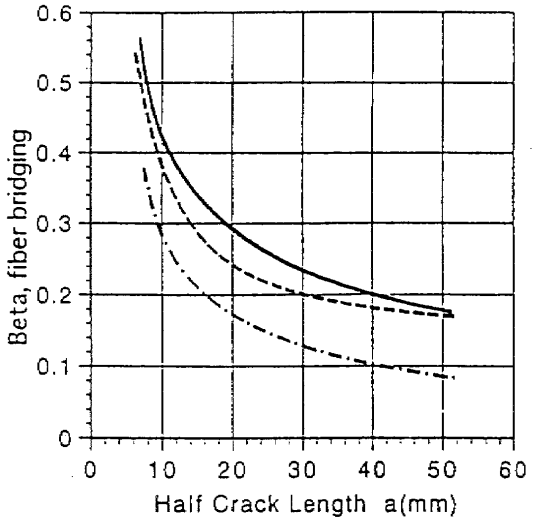

Glare 3 3/2 Glare 4 3/2 Glare 2 3/2

A	155.	-51.9	150.
B	-41.2	14.8	-33.4
C	6.09	1.58	4.68
D	.0720	.133	.0031

(Beta, fiber bridging)
$= A/(a^3) + B/(a^2) + C/a + D$

Figure 13 Best fit curves for 'β ,fiber bridging'

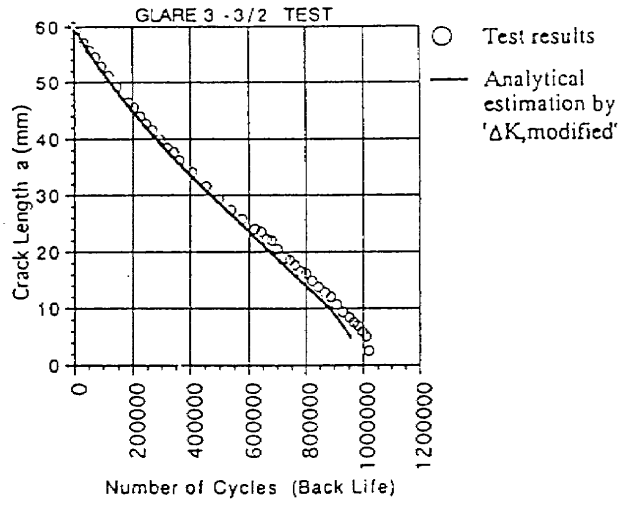

Figure 14 Crack growth simulation and comparison with test results